

We are IntechOpen, the world's leading publisher of Open Access books Built by scientists, for scientists

6,900

Open access books available

186,000

International authors and editors

200M

Downloads

Our authors are among the

154

Countries delivered to

TOP 1%

most cited scientists

12.2%

Contributors from top 500 universities



WEB OF SCIENCE™

Selection of our books indexed in the Book Citation Index
in Web of Science™ Core Collection (BKCI)

Interested in publishing with us?
Contact book.department@intechopen.com

Numbers displayed above are based on latest data collected.
For more information visit www.intechopen.com



One-Shot Phase-Shifting Interferometry with Phase-Gratings and Modulation of Polarization Using $N \geq 4$ Interferograms

Gustavo Rodríguez Zurita, Noel-Ivan Toto-Arellano
and Cruz Meneses-Fabián

*Benemérita Universidad Autónoma de Puebla,
México*

1. Introduction

Phase-shifting interferometry requires (PSI) of several interferograms of the same optical field with similar characteristics but shifted by certain phase values to retrieve the optical phase. This task has been usually performed by stages with great success and requires of a series of sequential shots [Meneses et al., 2006a]. However, time-varying phase distributions are excluded from this schema. Several efforts for single-shot phase-shifting interferometry have been tested successfully [Novak et al., 2005 ;Rodriguez et al., 2008a], but some of them require of non-standard components and they need to be modified in some important respects in order to get more than four interferograms. Two-windows grating interferometry, on the other hand, has been proved to be an attractive technique because of its mechanical stability as a common-path interferometer [Arrizón and De La Llave 2004]. Moreover, gratings can be used as convenient phase modulators because they introduce phase shifts through lateral displacements. In this regard, phase gratings offer more multiplexing capabilities than absorption gratings (more useful diffraction orders because higher diffraction efficiencies can be achieved). Furthermore, with two phase gratings with their vector gratings at 90° (grids) there appear even more useful diffraction orders [Toto et al., 2008]. Modulation of polarization can be independently applied to each diffraction order to introduce a desired phase-shift in each interference pattern instead of using lateral translations. These properties combine to enable phase-shifting interferometric systems that require of only a single-shot, thus enabling phase inspection of moving subjects. Also, more than four interferograms can be acquired that way. A simple interferogram processing enables the use of interference fringes with different fringe modulations and intensities. In this chapter, the basic properties of two-windows phase grating interferometry (TWPGI) and modulation of polarization is reviewed on the basis of the far-field diffraction properties of phase gratings and grids. Phase shifts in the diffraction orders can be used as an advantage because they simplify the needed polarization filter distributions. It is finally remarked, that these interferometers are compatible with interference fringes exhibiting spatial frequencies of relative low values and, therefore, no great loss of resolution is related with several interferograms when simultaneously using the same image field of the camera. To extract optical phase distributions which evolve in time, the capture of the n shifted

interferograms with one shot is desirable. Some approaches to perform this task have been already demonstrated [Wyant, 2004; Rodriguez et al., 2009], although only for $n = 4$ to our knowledge. Among these systems, the one using two windows in the object plane of a $4f$ system with a phase-grating in the Fourier plane and modulation of polarization (TWPGI) is a very simple possibility [Rodriguez 2008a]. In this communication, the capability of TWPGI to capture more than four interferograms in one shot is demonstrated with the introduction of a phase grid in place of the grating. To test TWPGI for more than four interferograms, the case of $n=(N+1)$ interferograms has been chosen. This method reduces errors in phase calculations when noisy interferograms are involved [Malacara D, 1998]. Experimental results for $n = 5, 7, 9$ interferograms are shown.

2. Experimental setup

A The Fig. 1 shows the arrangement of an ideal one-shot phase-shifting grating interferometer incorporating modulation of polarization. A combination of a quarter-wave plate Q and a linear polarizing filter P generates linearly polarized light at an appropriate azimuth angle (45°) entering the interferometer. Two quarter-wave plates (Q_L and Q_R) with their orthogonal fast axes are placed in front of the two windows of the common-path interferometer so as to generate left and right circularly polarized light as the corresponding beam leaves each window, see Fig. 1(a). A phase grating is placed at the system's Fourier plane as the pupil. In the image plane, Fig. 1(b) superimposition of diffraction orders result, causing replicated images to interfere.

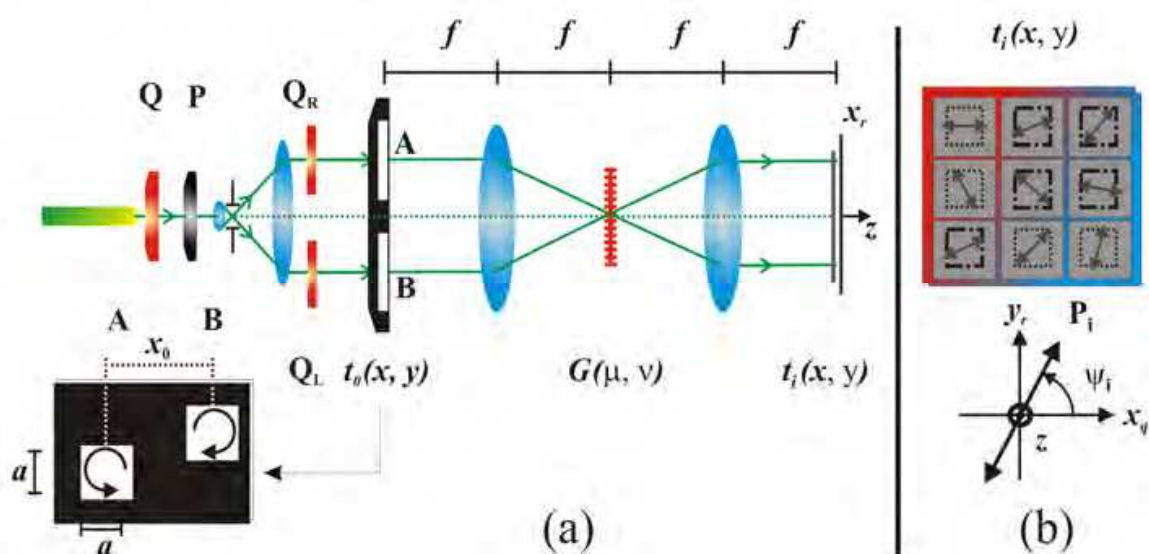


Fig. 1. (a) One-shot phase-shifting grating interferometer with modulation of polarization. A, B: windows. PBS: Polarizing Beam splitter; M_i : Mirrors; $G(\mu, \nu)$: Phase grid. (b) ψ_i : polarizing angles (with $i = 1, 2, 3, 4$ to obtain phase-shifts $\xi_i = 0^\circ, 90^\circ, 180^\circ, 270^\circ$ respectively). Translation of coordinates around the order position: $x_q = x - qF_0$ and $y_r = y - rF_0$. $\alpha' = 1.519$ rad.

The phase shifting ξ_i , $i = 1 \dots 4$, results after placing a linear polarizer to each one of the interference patterns generated on each diffracting orders in the exit plane (P_1, P_2, P_3, P_4).

Each polarizing filter transmission axis is adjusted at different angle ψ_i , so as to obtain the desired phase shift ξ_i for each pair of orders. For a 90° phase-shift ξ_i between interfering fields, the polarization angles ψ_i in each diffraction order must be 0° , 45° , 90° and 135° for the case of ideal quarter-wave retardation ($\alpha = 90^\circ$). In the next sections, some particularities arising from the optical components available for our set-up are discussed. Among these, the calculation of ψ_i for the case of a non exact quarter-wave retardation is considered through an example.

3. Interference patterns with polarizing filters and retarding plates

3.1 Phase grids

Object and image planes are described by (x, y) coordinates. A periodic phase-only transmittance $G(u, v)$ is placed in the frequency plane (u, v) . Then $\mu = u/\lambda f$ and $v = v/\lambda f$ are the frequency coordinates scaled to the wavelength λ and the focal length f . In the plane (u, v) , the period of G is denoted by d (the same in both axis directions) and thus, its spatial frequency by $\sigma = 1/d$. Two neighboring diffraction orders have a distance of $X_0 = \lambda f/d$ in the image plane. Then, $\sigma \cdot u = X_0 \cdot \mu$. Taking the rulings of one grating along the μ direction and the rulings of the second grating along the ν direction, the resulting centered phase grid can be written as

$$G(\mu, \nu) = e^{i2\pi A_g \sin[2\pi \cdot X_x \mu]} e^{i2\pi A_g \sin[2\pi \cdot X_y \nu]} = \sum_{q=-\infty}^{\infty} J_q(2\pi A_g) e^{i2\pi \cdot q X_0 \mu} \sum_{r=-\infty}^{\infty} J_r(2\pi A_g) e^{i2\pi \cdot r X_0 \nu} \quad (1)$$

where the frequencies along each axes directions are taken of the same value. The Fourier transform of the phase grid becomes

$$\tilde{G}(x, y) = \sum_{q=-\infty}^{\infty} \sum_{r=-\infty}^{\infty} J_q(2\pi A_g) J_r(2\pi A_g) \delta(x - qX_0, y - rX_0) \quad (2)$$

which consists of point-like diffraction orders distributed in the image plane on the nodes of a lattice with a period given by X_0 .

3.2 Two-window phase-grating interferometry: fringe modulation

Phase grating interferometry is based on a phase grating placed as the pupil of a $4f$ Fourier optical system [Rodriguez et al., 2008a; Thomas and Wyant, 1976]. The use of two windows at the object plane in conjunction with phase grating interferometry allows interference between the optical fields associated to each window with higher diffraction efficiency [Arrizon and Sanchez, 2004; Ramijan, 1978]. Such a system performs as a common path interferometer (Fig. 1). When using birefringent plates which do not perform exactly as quarter-wave plates for the wavelength employed, the polarization angles of the linear polarizing filters to obtain 90° phase-shifts must change [Rodriguez et al., 2008a].

To calculate the phase shifts induced in a more general polarization states by linear polarizers, consider two fields whose Jones vectors are described respectively by

$$\vec{J}_L(x, y) = \frac{1}{\sqrt{2}} \begin{pmatrix} 1 \\ e^{i\alpha'} \end{pmatrix} \quad \vec{J}_R(x, y) = \frac{1}{\sqrt{2}} \begin{pmatrix} 1 \\ e^{-i\alpha'} \end{pmatrix}, \quad (3)$$

These vectors represent the polarization states of two beams emerging from a retarding plate with phase retardation $\pm\alpha'$. Each beam enters the plate with linear polarization at $\pm 45^\circ$ with respect to the plate fast axis. Due to their orientations, the electric fields of the beams rotate in opposite directions, thereby the indices L and R . A convenient window pair for a grating interferometer implies an amplitude transmittance given by

$$\vec{t}_0(x, y) = \vec{J}_L \cdot w\left(x - \frac{x_0}{2}, y - \frac{y_0}{2}\right) + \vec{J}_R w'\left(x + \frac{x_0}{2}, y + \frac{y_0}{2}\right), \quad (4)$$

and x_0 and y_0 give the mutual separations between the centers of each window along the coordinate axis. One rectangular aperture can be written as $w(x, y) = \text{rect}[x/a] \cdot \text{rect}[y/b]$ whereas the second one, as $w'(x, y) = w(x, y) \exp\{i\phi(x, y)\}$, a relative phase between the windows being described with the function ϕ . a represents the side length of each window. The image $\vec{t}_i(x, y)$ formed by the system consists basically of replications of each window at distances X_0 , that is, the convolution of $\vec{t}_0(x, y)$ with the point spread function of the system, defined by the inverse Fourier transform of

$$\tilde{\Gamma}_2(\mu, \nu) = \frac{1}{2} \begin{pmatrix} 1 & 0 \\ 0 & 1 \end{pmatrix} G_2(\mu, \nu). \quad (5)$$

This results into the following

$$\begin{aligned} \vec{t}_f(x, y) &= \vec{t}_2(x, y) * \mathfrak{T}^{-1}\{\tilde{\Gamma}_2(\mu, \nu)\} \\ &= \frac{1}{2} \begin{pmatrix} 1 & 0 \\ 0 & 1 \end{pmatrix} \cdot \vec{t}_2(x, y) * \mathfrak{T}^{-1}\{\tilde{G}_2(\mu, \nu)\}. \end{aligned} \quad (6)$$

Assuming $y_0 = x_0$, by invoking the condition of matching first-neighboring orders, $X_0 = x_0$, $q' = q + 1$ and $r' = r + 1$, and the image is then basically described by

$$\begin{aligned} \vec{t}_0(x, y) * \tilde{G}(x, y) &= \\ &\vec{J}_L \sum_{q, r} J_q J_r \cdot w\left(x - \left(q + \frac{1}{2}\right)x_0, y - \left(r + \frac{1}{2}\right)x_0\right) \\ &+ \vec{J}_R \sum_{q', r'} J_{q'} J_{r'} \cdot w'\left(x - \left(q' + \frac{1}{2}\right)x_0, y - \left(r' + \frac{1}{2}\right)x_0\right) = \\ &\sum_{q=-\infty}^{\infty} \sum_{r=-\infty}^{\infty} \left\{ \vec{J}_L J_q J_r + \vec{J}_R J_{q+1} J_{r+1} \cdot \exp\left[i\phi\left(x - \left(q + \frac{1}{2}\right)x_0, y - \left(r + \frac{1}{2}\right)x_0\right)\right] \right\} \end{aligned} \quad (7)$$

where some inessential constants are dropped. By selecting the diffraction term of order qr , after placing a linear polarizing filter with transmission axis at the angle ψ , \vec{J}_ψ^L , its irradiance results proportional to

$$\left\| \vec{J}_L' J_q J_r + \vec{J}_R' J_{q+1} J_{r+1} \cdot \exp[i\phi(x', y')] \right\|^2 = A(\psi, \alpha') \cdot \left[(J_q J_r)^2 + (J_{q+1} J_{r+1})^2 + 2 J_q J_r J_{q+1} J_{r+1} \cdot \cos[\xi(\psi, \alpha') - \phi(x', y')] \right], \tag{8}$$

with

$$\vec{J}_\psi^L = \begin{pmatrix} \cos \psi & -\sin \psi \\ \sin \psi & \cos \psi \end{pmatrix}, \quad \vec{J}_L' = J_\psi^L \vec{J}_L, \quad \vec{J}_R' = J_\psi^L \vec{J}_R, \tag{9}$$

and also [4]

$$A(\psi, \alpha') = 1 + \sin(2\psi) \cdot \cos(\alpha'), \quad \xi(\psi, \alpha') = \text{ArcTan} \left[\frac{\sin(\alpha')}{\frac{\cot(2\psi)}{1 + \tan(\psi) \cdot \cos(\alpha')} + \cos(\alpha')} \right]. \tag{10}$$

Plots of $\xi(\psi, \alpha')$ and $A(\psi, \alpha')$ are shown in Fig. 2 for several values of α' .

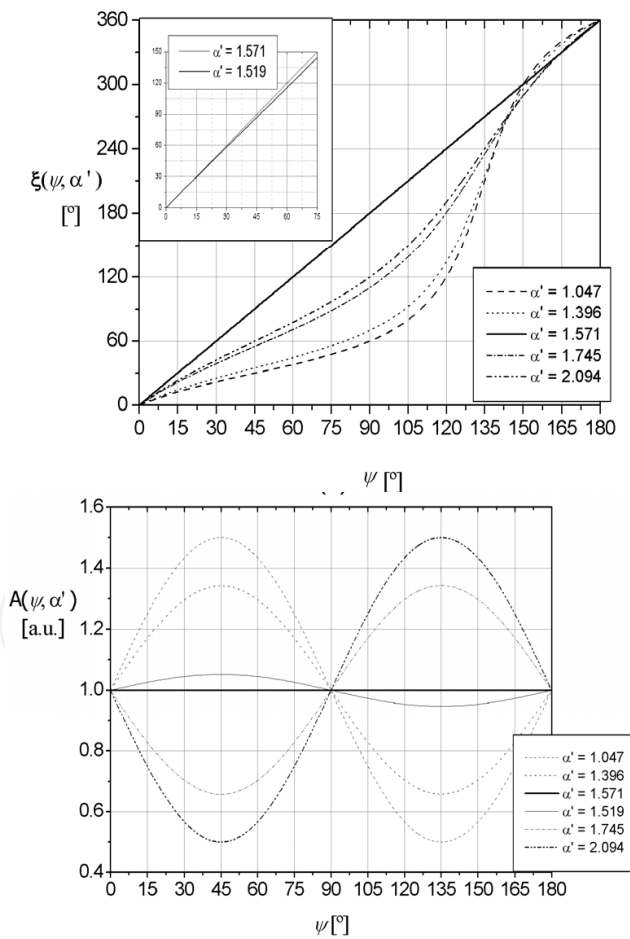


Fig. 2. (a) Phase shift $\xi(\psi, \alpha')$ as a function of ψ for several values of α' . Insert: α' for ideal retardation and experimental retardation. (b) Amplitude $A(\psi, \alpha')$ as a function of ψ for several values of α' .

Thus, an interference pattern between fields associated to each window must appear within each replicated window. It is shifted by an amount ξ induced by polarization. For the case of exact quarter-wave retardation, $A(\psi, \pi/2)=1$ and $\xi(\psi, \pi/2)=2\psi$. Otherwise, these quantities must be evaluated with Eqs. (8). The fringe modulation m_{qr} of each pattern would be of the form

$$m_{qr} = \frac{2J_q J_{q-1} J_r J_{r-1}}{J_q^2 J_r^2 + J_{q-1}^2 J_{r-1}^2} \quad (11)$$

The Fourier spectrum of the grid in our tests behaves as sketched in Fig. 3, where two equal phase gratings are shown with their respective $+4^{\text{th}}$ diffraction order assumed negative [Fig. 3(a)]. Thus, the -4^{th} diffraction order results also negative. A phase grid is formed with the gratings at 90° and the resulting Fourier spectrum forms a rectangular reticule [Fig. 3(b)]. Due to the π phase difference between orders, there are orders pointing out toward the reader (circles) or away (crosses). Because the window are displaced, two Fourier spectra become shifted from the origin diagonally and in opposite directions [Fig. 3(c)]. Similar rows and columns are encircled within the dotted lines. Under our matching condition, the order qr superimposes with the order $(q-1)(r-1)$. Thus, some orders are in phase (dots with dots or crosses with crosses, but only one symbol depicted) and others out of phase (dot with cross). Then, only one symbol means positive contrast, while both symbols mean contrast reversal [Fig. 3(c)].

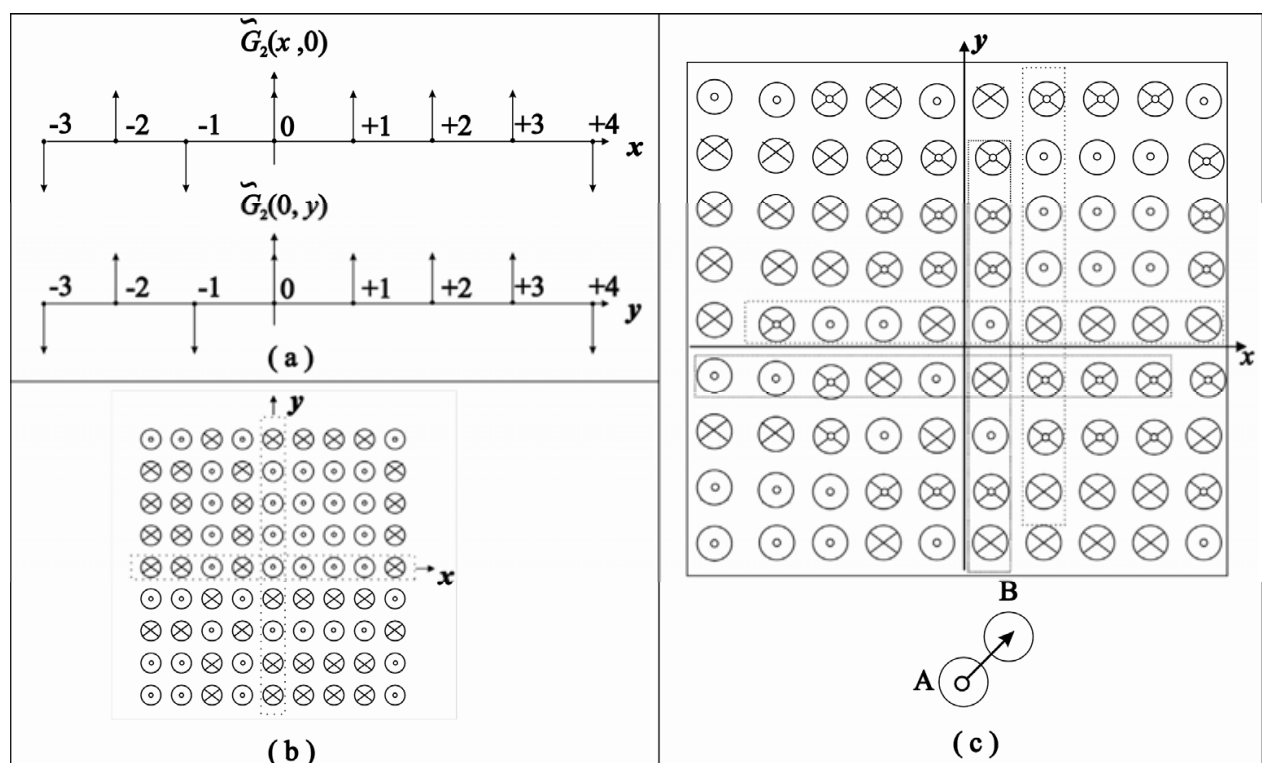


Fig. 3. a) One dimensional spectra of identical phase gratings to be crossed in order to construct a grid. b) Corresponding image plane for the phase grid. c) Two shifted Fourier spectra are superimposed according to the windows displacement A-B.

4. Experimental testing of the phase-shifts in phase grids

For the case of the diffractions orders belonging to a phase-grid constructed with two crossed gratings of equal frequency, the corresponding interference patterns are shown in Fig.4. Each grating gives patterns as in Fig. 4(a) when placed alone in the system of Fig. 1 with no plate retarders neither linear polarizing filters. The whole figure is a composite image because patterns of higher order have lower intensities. The fringe modulation signs are in agreement with the conclusions derived from Fig. 2. The relative phase values of the 16 patterns within the square (drawn with dotted lines in the patterns of Fig. 4) employing the method from Kreis, 1986 can be seen in Table 1.

Any grating displacement on its plane only introduces a constant phase term in Eqs. (6) and (8) which, in turn, only shifts each interference pattern by the same amount independent of the diffraction order [Arrizon and Sanchez 2004; Meneses et al., 2006b]. Modulation of polarization employed to attain the needed shifts in each interferogram is described in the next sections taking only four of 16.

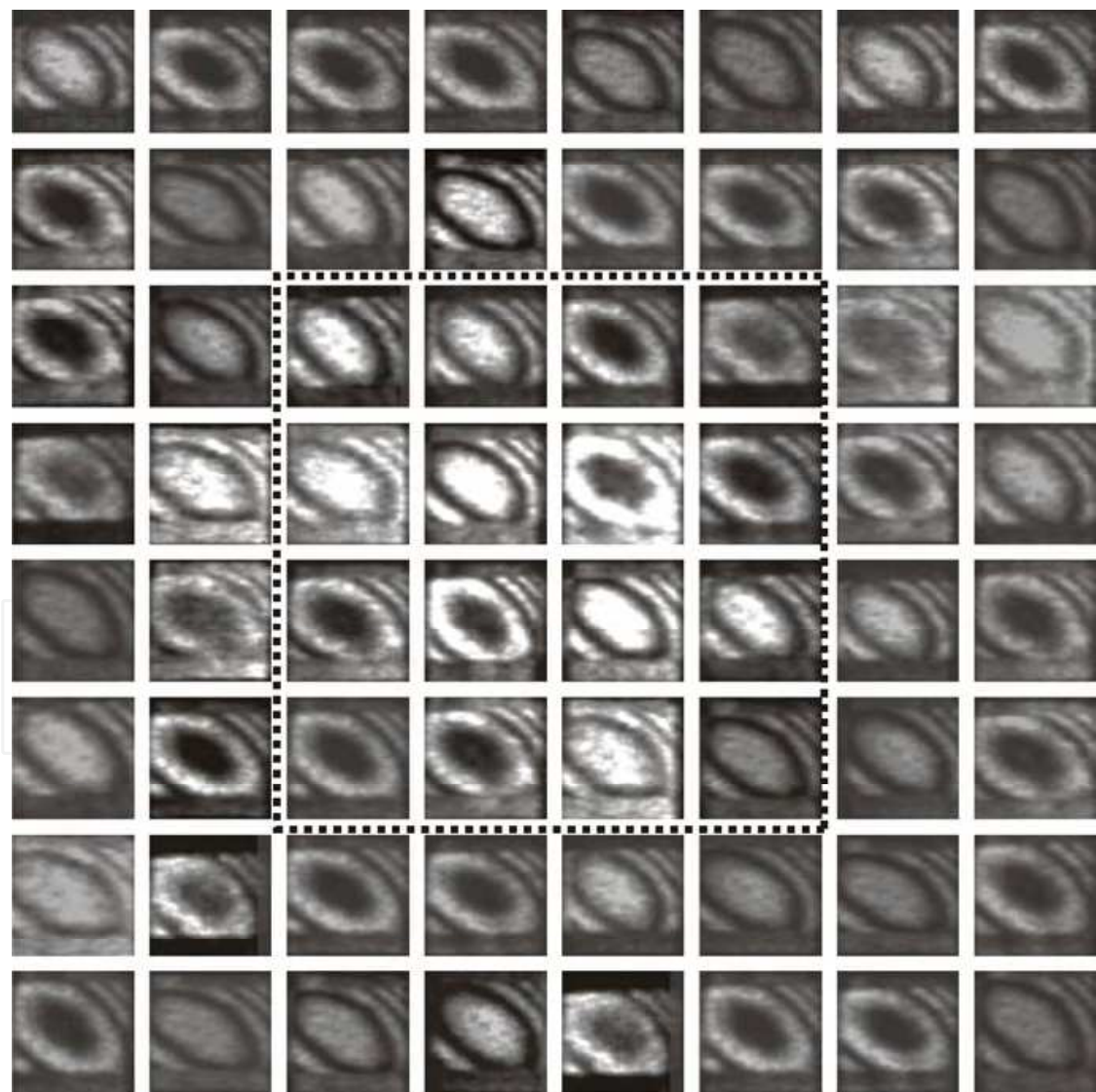


Fig. 4. Experimental patterns for a phase-grid.

Shifts (rad)			
0.016	0.040	3.129	3.173
0.009	0.016	3.150	3.187
3.144	3.173	0.000	0.010
3.137	3.122	0.017	0.037

Table 1. Phase shifts of the 16 patterns within the dotted square of Fig. 3, as measured by the method from Kreis 2986.

5. Phase-grid interference patterns with modulation of polarization

Incorporating modulation of polarization, a TWPGI can be used for dynamic interferometry. This system is able to obtain four interferograms 90° phase-apart with only one shot. Phase evolving in time can then be calculated and displayed on the basis of phase-shifting techniques with four interferograms. The system performs as previous proposals to attain four interferograms with a single shot [Barrientos et al., 1999; Novak et al., 2005]. In the following sections, a variant of a TWPGI able to capture $N \geq 4$ interferograms in one shot is described. It consists of the set-up shown in Fig. 1. The system uses a grid as a beam splitter in a way that resembles the well-known double-frequency shearing interferometer as proposed by Wyant,2004, but our proposal differs from it not only because of its modulation of polarization, the use of a single frequency and the use of two windows, but also in the phase steps our system introduces. Besides, ours is not a shearing interferometer of any type.

The Fig. 1 shows the arrangement of a one-shot phase-shifting grid interferometer including modulation of polarization with retarders for the windows and linear polarizers on the image plane. The system generates several diffraction orders of similar irradiances in the average but not equal fringe modulations, as expected. Each interferogram image was scaled to the same values of grey levels (from 0 to 255). Previous reports show that a simplification for the polarizing filters array can be attained when using the phase shifts of π [10] to obtain values of ξ of 0, $\pi/2$, π and $3\pi/2$, due to the π -shifts, only two linear polarizing filters have to be placed (instead of four filters, without the π -shifts). The transmission axes of the filter pairs P_1 , P_3 and P_2 , P_4 can be the same for each as long as they cover two patterns 180° phase apart (Fig. 4). The needed values of ψ have to be of $\psi_1=0^\circ$ and $\psi_2=45^\circ$ with ideal quarter-wave retarders. But considering the retarders at disposal, it can be shown with Eq. (10) that ψ can be of $\psi_1=0^\circ$ and $\psi_2=46.577^\circ$. They are sketched in Fig. 4. The square enclosing the 16 windows replicas in the same figure is to be compared with the similar square of Fig. 5 (dotted lines).

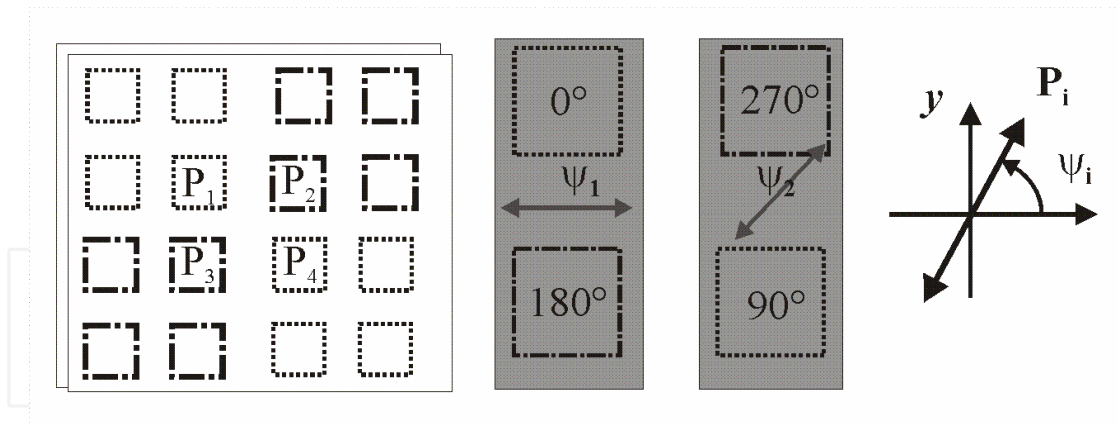


Fig. 5. Polarizing filters array for 90° phase stepping.

5.1 Case of four interferograms

For phase-shifting interferometry with four patterns, four irradiances can be used, each one taken at a different ψ angle. The relative phase can be calculated as [Schwieder, 1983]

$$\tan \phi = \frac{\|\bar{J}_1\|^2 - \|\bar{J}_3\|^2}{\|\bar{J}_2\|^2 - \|\bar{J}_4\|^2} \tag{12}$$

where $\|\bar{J}_1\|^2$, $\|\bar{J}_2\|^2$, $\|\bar{J}_3\|^2$ and $\|\bar{J}_4\|^2$ are the intensity measurements with the values of ψ such that $\xi(\psi_1)=0, \xi(\psi_2)=\pi/2, \xi(\psi_3)=\pi, \xi(\psi_4)=3\pi/2$ respectively. Note that $\xi(\psi, \pi/2)=2\psi$ and $A(\psi, \pi/2)=1$, so a good choice for the retarders is quarter-wave retarders, as is well known. Dependence of ϕ on the coordinates of the centered point has been simplified to x,y . The same fringe modulation m_q results as in Eq. (8). Therefore, the discussion about fringe modulation given in previous sections is retained when introducing the modulation of polarization. Such polarization modulation can be made also for grids, resulting in similar conclusions.

5.2 Case of five, seven, and nine interferograms

To demonstrate the use of the several interferograms obtained to extract phase under the conditions as described above, we choose the symmetrical N+1 phase steps algorithms for data processing in the cases N= 4, 6, 8. The phase for N shifts is given by [Malacara, 1998]:

$$\tan \phi(x,y) = \frac{\sum\limits_i^{N+1} I_i \sin\left(2\pi \frac{i-1}{N}\right)}{\sum\limits_i^{N+1} I_i \cos\left(2\pi \frac{i-1}{N}\right)} \tag{13}$$

where N+1 is the number of interferograms. The Fig. 6 shows the polarizing filters employed. For the case of five interferograms, only three linear polarizing filters have to be placed. The transmission axes of the filter pairs P_n can be the same for each as long as they cover two patterns with 180° phase shift in between.

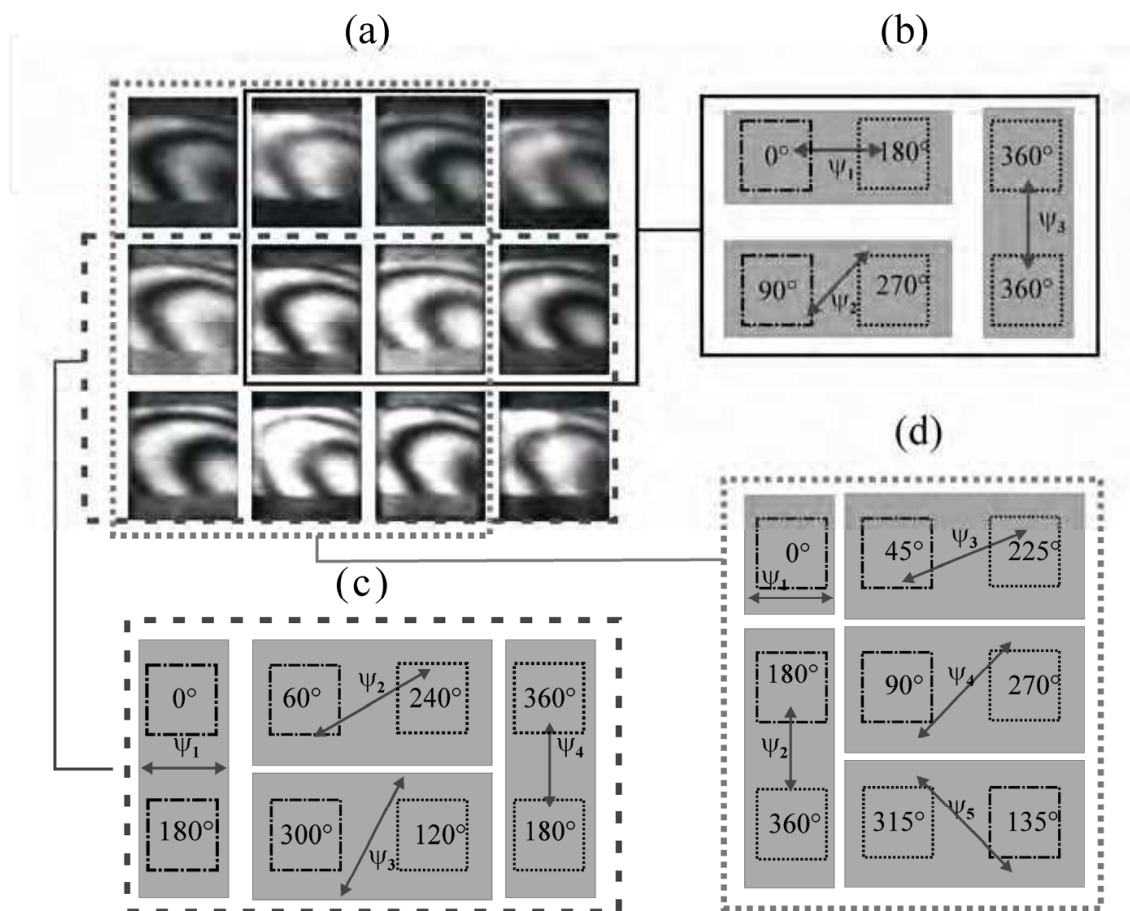


Fig. 6. Polarizing filters array for five, seven and nine interferograms. a) 12 interference patterns detected with a polarizing filter at $\psi=35^\circ$ covering all of them. Some π -shifts can be recognized when reversal contrasts are present. b) $N=4$, symmetrical five. c) $N=6$, symmetrical seven. d) $N=8$, symmetrical nine.

6. Experimental results

Two objects for testing are a phase disk and a phase step. When each object was placed separately in one of the windows using the TWPGI with the polarizers array, the interferograms of Fig. 7 were obtained. For each object, the four interferograms are shown together with the calculated unwrapped phase. However, more than four interferograms could be used, whether for N -steps phase-shifting interferometry [Shwieder et al., 1983] or for averaging images with the same shift. Examples, some typical raster lines for each unwrapped phase are shown in Fig. 8 (in arbitrary phase units).

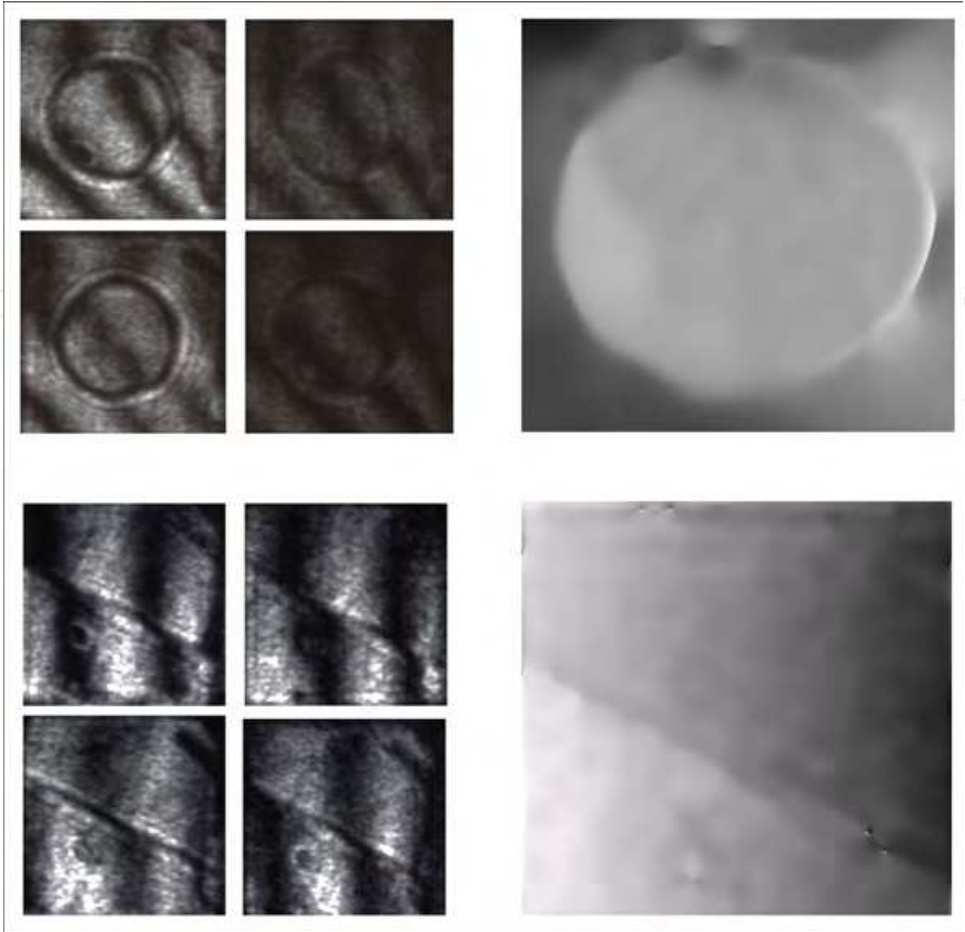


Fig. 7. Upper row: phase dot. Four 90° phase-shifted interferograms and unwrapped phase. Lower row: phase step. Four 90° phase-shifted interferograms and unwrapped phase.

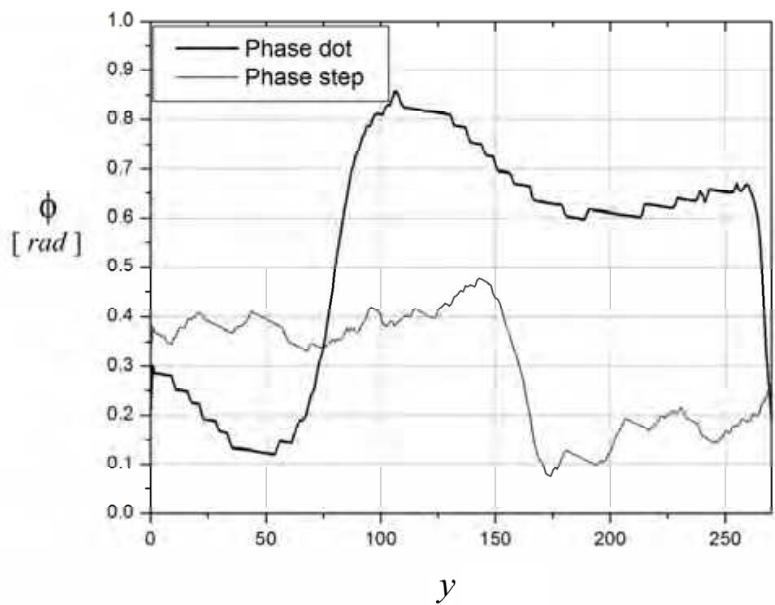


Fig. 8. Unwrapped calculated phases along typical raster lines of each object of Fig. 5. Scale factor : 0.405 rad.

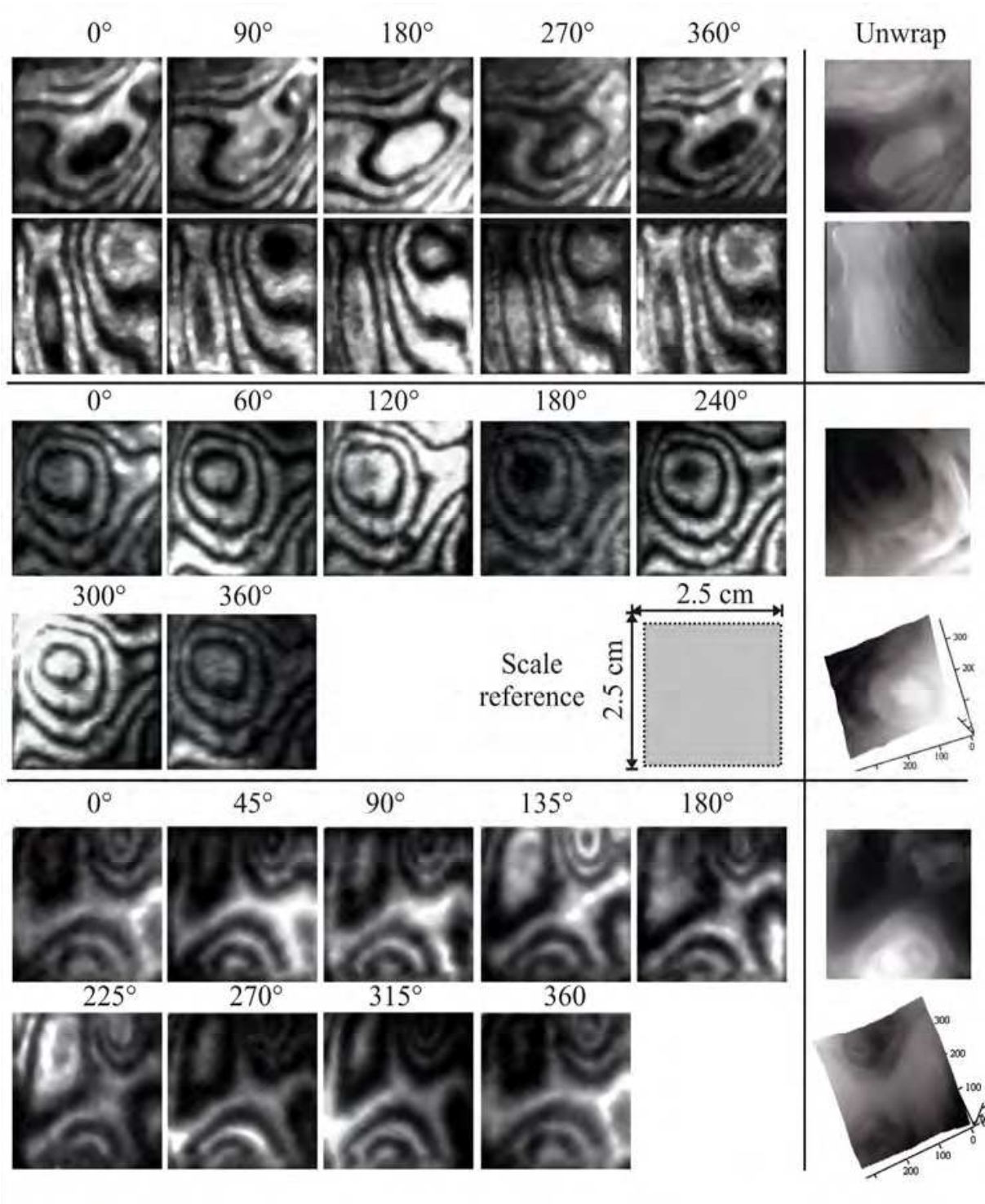


Fig. 9. Flow of oil drops on glass. Phase-shifted interferograms and unwrapped phases. Upper two rows: two examples of five 90° phase-shifts. Center rows: seven 60° phase-shifts. Lower rows: nine 45° phase-shifts. Reference square for scale dimensions.

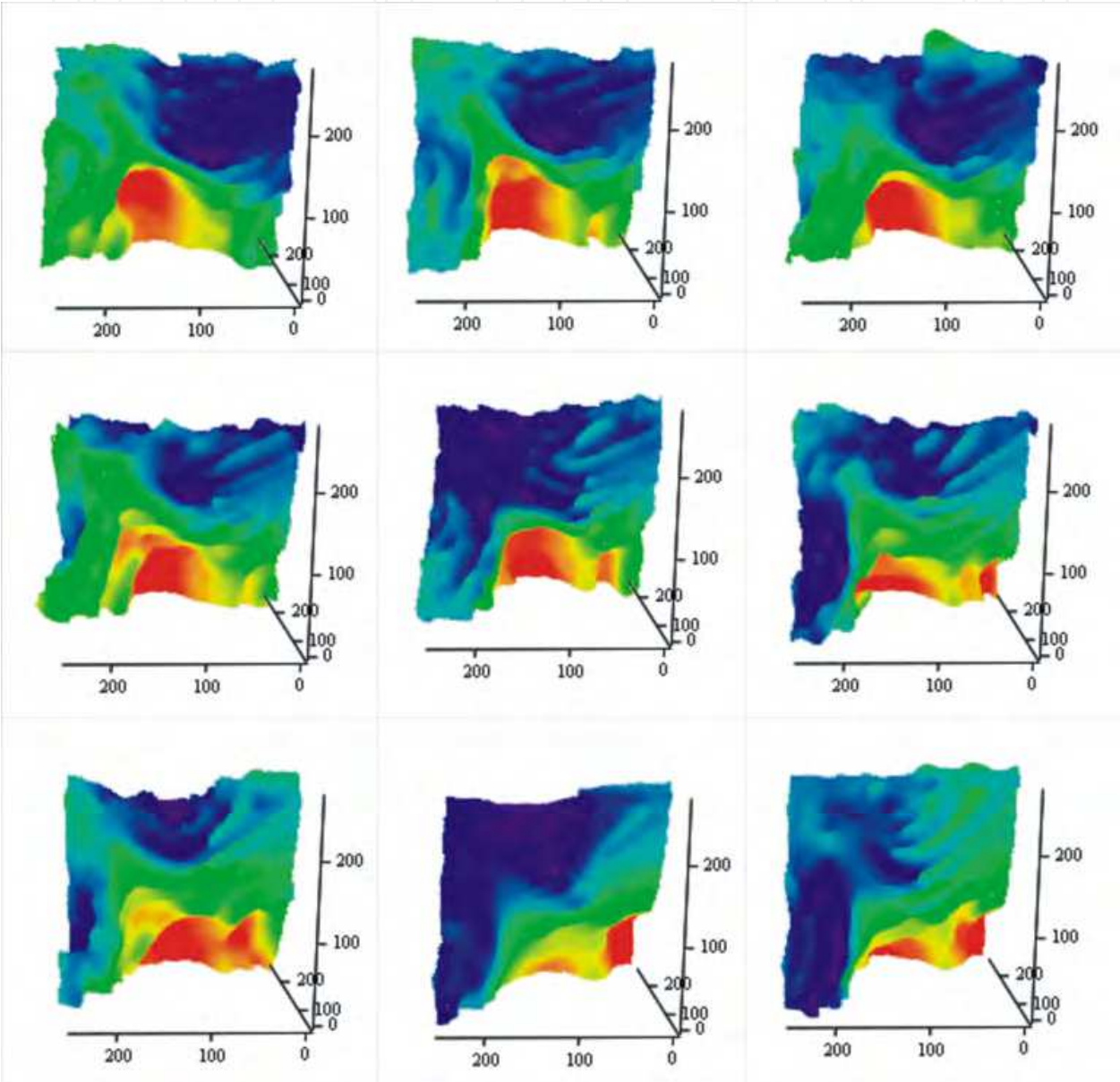


Fig. 10. Typical frames from an unwrapped phase from interferograms of oil flowing.

Considering the retarders at disposal, according to Eq. (10) it can be shown that ψ_n can be of $\psi_1 = 0^\circ$, $\psi_2 = 46.577^\circ$ and $\psi_3 = 92.989^\circ$, each step ξ being of 90° . For the case of symmetrical seven, each step ξ is of 60° , so it can be shown that ψ_n are $\psi_1 = 0^\circ$, $\psi_2 = 30.800^\circ$, $\psi_3 = 62.330^\circ$ and $\psi_4 = 92.989^\circ$. For symmetrical nine, $\psi_1 = 0^\circ$, $\psi_2 = 92.989^\circ$, $\psi_3 = 22.975^\circ$, $\psi_4 = 46.577^\circ$ and $\psi_5 = 157.903^\circ$. In this case, each step ξ has to be 45° . The corresponding results are shown in Fig. 9, where the object was an oil drop running down over a microscope slide. Each interferogram was subject to rescaling and normalization and then, a filtering process prior to phase calculation through Eq. (13).

6.1 Moving distributions

Immersion oil was applied to a glass microscope slide and allowed to flow under the effect of gravity by tilting the slide slightly. The slide was put in front of one of the object windows of the system of Fig. 1. Fig. 10 shows the resulting unwrapped phase evolution of oil flow (Case N=4).

7. Final remarks

The experimental set-up for a polarizing two-window phase-grating common-path interferometer has been described. This system is able to obtain four interferograms 90° phase-apart in only one shot. Therefore, it is suitable to carry out phase extraction using phase shifting techniques. Phase evolving in time can then be calculated and displayed. The system is considerably simpler than previous proposals to attain four interferograms with only one shot. In its present form, it is, however, best suited to relative small objects which do not introduce polarization changes. Because it works with interferograms placed relatively far from the optical axes, experimental results suggest that some method has to be introduced to compensate mainly for distortion, among other off-axis aberrations. This compensation could be optical (as a better design of the optical imaging system) or digital (fringe distortion compensation by inverse transformation). In the experiments, the use of is described retarding plates which are not quarter-wave plates. Although they can perform well enough in principle, it seems better to use quarter-wave plates because no additional variations of the interferogram amplitude arise. Also in this case, a simpler polarization filter array can be used taking advantage of the diffraction properties of a phase grating. Some special phase gratings design could optimize the interferometric system described.

This system is able to obtain $n = (N+1)$ interferograms with only one shot ($n \leq 16$). Tests with $2\pi / N$ phase-shifts were presented, but other approaches using different phase-shifts could be attained using linear polarizers with their transmission axes at the proper angle before detection. The phase shifts of π due to the grid spectra allows the use of a number of polarizing filters which is less than the number of interferograms, simplifying the filter array. Other configurations for the window positions which are different as the one reported in this communication can also be possible. The accuracy in measurements is the one typical of phase-shifting. Some trade-offs appear while placing several images over the same detector field, but for low frequencies interferograms (with respect to the inverse of the pixel spacing) the influence of these factors seems to be rather small if noticeable. The interferometer could be used for objects with no changes of polarization.

8. Acknowledgements

Partial support from Benemérita Universidad Autónoma de Puebla (BUAP), project: 154984 (CONACYT-BUAP) is also acknowledged. Author N.-I. Toto-Arellano expresses sincere appreciation to Luisa, Miguel and Damian for the support provided, and to CONACYT for grant 102137/43055.

9. References

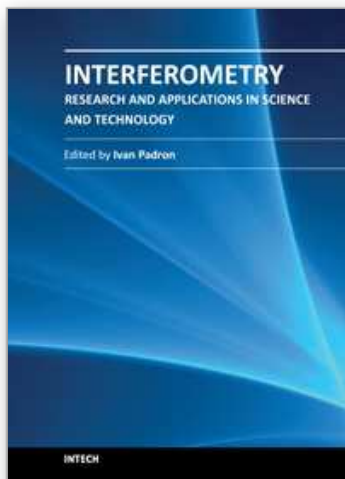
- Arrizón V. and Sánchez-De-La-Llave D., (2004). Common-Path Interferometry with One-Dimensional Periodic Filters, *Opt. Lett.* Vol. 29, pp. 141-143.
- Barrientos-García B., Moore A. J., Pérez-López C., Wang L., and Tschudi T., (1999) Spatial Phase-Stepped Interferometry using a Holographic Optical Element, *Opt. Eng.* Vol. 38, pp. 2069-2074
- Malacara D., Servin M., and Malacara Z.; Marcel Dekker (1998). *Interferogram Analysis for Optical Testing*.
- Meneses-Fabian C., Rodríguez-Zurita G., and Arrizon V. (2006a). Common-Path Phase-Shifting Interferometer with Binary Grating, *Opt. Commun.* Vol. 264, pp. 13-17.
- Meneses-Fabian C., Rodríguez-Zurita G., and Arrizon V., (2006b). Optical Tomography of Transparent Objects with Phase-Shifting Interferometry and Stepping-Wise Shifted Ronchi Ruling, *J. Opt. Soc. Am. A*, Vol. 23, pp. 298-305.
- Novak M., Millerd J., Brock N., North-Morris M., Hayes J. and Wyant J.C., (2005). Analysis of a micropolarizer array-based simultaneous phase-shifting interferometer, *Appl. Opt.*, Vol. 44, pp. 6861-6868.
- Kreis T., (1986). Digital Holographic Interference-Phase Measurement Using the Fourier-Transform Method, *J. Opt. Soc. Am. A*, Vol. 3, pp. 847-855.
- Rodríguez-Zurita G., Meneses-Fabian C., Toto-Arellano N., Vázquez-Castillo J. F. and Robledo-Sánchez C., (2008). One-Shot Phase-Shifting Phase-Grating Interferometry with Modulation of Polarization: case of four interferograms, *Opt. Express*, Vol. 16, 7806-7817.
- Rodríguez-Zurita G., Toto-Arellano N. I., Meneses-Fabian C. and Vázquez-Castillo J. F., (2008). One-shot phase-shifting interferometry: five, seven, and nine interferograms, *Opt Letters*, Vol. 33, pp. 2788-2790.
- Rodríguez-Zurita G., Toto-Arellano N. I., Meneses-Fabian C. and Vázquez-Castillo J. F., (2009). Adjustable lateral-shear single-shot phase-shifting interferometry for moving phase distributions, *Meas. Sci. Technol.* Vol. 20, pp. 115902.
- Schwieder J., Burow R., Elssner K.-E., Grzanna J., Spolaczyk R. and Merkel K., (1983). Digital Wave-Front Measuring Interferometry: some systematic error sources, *Appl. Opt.*, Vol. 22, pp. 3421-3432.
- Thomas D. A., and Wyant J. C., (1976). High Efficiency Grating Lateral Shear Interferometer, *Opt. Eng.*, Vol. 15, pp. 477.
- Toto-Arellano N. I., Rodríguez-Zurita G., Meneses-Fabian C., Vazquez-Castillo J. F., (2008). Phase shifts in the Fourier spectra of phase gratings and phase grids: an application

for one shot phase-shifting interferometry, Opt. Express, Vol. 16, pp. 19330-19341

Wyant J.C. (2004). Vibration insensitive interferometric optical testing, in Frontiers in Optics, OSA Technical Digest, OTuB2.

IntechOpen

IntechOpen



Interferometry - Research and Applications in Science and Technology

Edited by Dr Ivan Padron

ISBN 978-953-51-0403-2

Hard cover, 462 pages

Publisher InTech

Published online 21, March, 2012

Published in print edition March, 2012

This book provides the most recent studies on interferometry and its applications in science and technology. It is an outline of theoretical and experimental aspects of interferometry and their applications. The book is divided in two sections. The first one is an overview of different interferometry techniques and their general applications, while the second section is devoted to more specific interferometry applications comprising from interferometry for magnetic fusion plasmas to interferometry in wireless networks. The book is an excellent reference of current interferometry applications in science and technology. It offers the opportunity to increase our knowledge about interferometry and encourage researchers in development of new applications.

How to reference

In order to correctly reference this scholarly work, feel free to copy and paste the following:

Gustavo Rodríguez Zurita, Noel-Ivan Toto-Arellano and Cruz Meneses-Fabián (2012). One-Shot Phase-Shifting Interferometry with Phase-Gratings and Modulation of Polarization Using $N \geq 4$ Interferograms, Interferometry - Research and Applications in Science and Technology, Dr Ivan Padron (Ed.), ISBN: 978-953-51-0403-2, InTech, Available from: <http://www.intechopen.com/books/interferometry-research-and-applications-in-science-and-technology/one-shot-phase-shifting-interferometry-with-phase-gratings-and-modulation-of-polarization-using-n-4->

INTECH
open science | open minds

InTech Europe

University Campus STeP Ri
Slavka Krautzeka 83/A
51000 Rijeka, Croatia
Phone: +385 (51) 770 447
Fax: +385 (51) 686 166
www.intechopen.com

InTech China

Unit 405, Office Block, Hotel Equatorial Shanghai
No.65, Yan An Road (West), Shanghai, 200040, China
中国上海市延安西路65号上海国际贵都大饭店办公楼405单元
Phone: +86-21-62489820
Fax: +86-21-62489821

© 2012 The Author(s). Licensee IntechOpen. This is an open access article distributed under the terms of the [Creative Commons Attribution 3.0 License](https://creativecommons.org/licenses/by/3.0/), which permits unrestricted use, distribution, and reproduction in any medium, provided the original work is properly cited.

IntechOpen

IntechOpen